Progress in Brain Research, Vol. 147
ISSN 0079-6123

CHAPTER 6

Biologically plausible models of neurite outgrowth

Gregor Kiddie[1,*], Douglas McLean[1], Arjen Van Ooyen[2] and Bruce Graham[1]

[1]*Department of Computing Science and Maths, Stirling University, Stirling, Stirlingshire, FK9 4LA, UK*
[2]*Netherlands Institute for Brain Research, Meibergdreef 33, 1105 AZ Amsterdam, The Netherlands*

Introduction

Mathematical modeling and computer simulation are valuable tools in unravelling the complexities underlying the morphological development of neurons. In this chapter, we consider biologically plausible mathematical models of neurite initiation, elongation, and branching. These models attempt to describe the intra- and extracellular environments of a developing neuron and determine the limiting factors in neurite outgrowth. This typically involves modeling the production, degradation, and transport of one or more chemicals in one or two spatial dimensions. For example, the one-dimensional diffusion and active transport of tubulin within a neurite, or the two-dimensional diffusion gradient of a chemoattractant in the external environment surrounding a neuron grown in cell culture. Extension to three dimensions to accurately describe neuronal growth in vivo may be desirable, but is highly computationally intensive and likely analytically intractable. The numerical solution of even one- or two-dimensional models is computationally demanding and requires considerable care in specifying appropriate temporal and spatial discretization. As the neuronal morphology changes over time so must the spatial discretization representing the neuron also change. Numerical techniques that address this issue are described.

*Corresponding author. Tel.: +44 1786 467421; Fax: +44 1786 464551; E-mail: gak@cs.stir.ac.uk

Neurobiology of neurite outgrowth

Neuronal growth happens in several stages. Firstly, wave-like extensions of the cell membrane, known as lamellipodia, develop into short neurites (neurite initiation) (Dotti et al., 1988; Dehmelt and Halpain, 2004). During a period of outgrowth and retraction of these neurites, one comes to dominate and elongates rapidly while inhibiting the outgrowth of the remaining neurites (neurite differentiation). This neurite becomes the axon and assumes distinct molecular characteristics. Following this, the dendritic arbor is elaborated through the elongation and branching of the remaining neurites. Initially, the arbor grows rapidly, with respect to total dendritic length, and the arborization changes repeatedly. Eventually, the rate of elongation slows down, and the shape of the arbor changes less (Wong and Wong, 2000; Cline, 2001). Rapid changes in neurite arborization are the result of the high rate at which a neurite extends and retracts small branches. This rate of addition and subtraction slows drastically as the neurite matures. Synapse formation and electrical activity may result in both the stabilization of particular neurite branches and the enhancement of outgrowth of new branches at different stages of neurite development (Cline, 2001; Wong and Wong, 2002).

Fundamental to neurite initiation, elongation and branching are the dynamics of the intracellular cytoskeletons (see Fig. 1). The complex growth cone at the tip of a growing neurite contains an actin

DOI: 10.1016/S0079-6123(04)47006-X

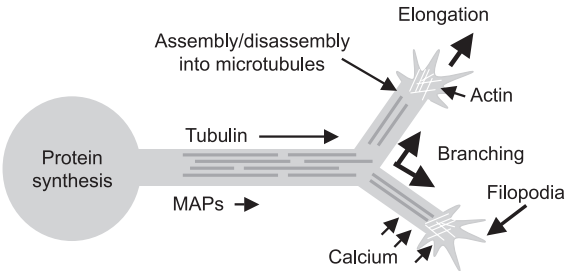

Fig. 1. Internals of a growing neurite.

cytoskeleton which is influenced by extracellular signals via protruding filopodia. The trailing neurite contains a rigid microtubule cytoskeleton. Assembly of tubulin into microtubules is required for neurite elongation. The stability of both the actin and microtubule cytoskeletons, which is determined by many intracellular proteins and extracellular signals (Acebes and Ferrus, 2000; Redmond and Ghosh, 2001; Whitford et al., 2002), influences the propensity of a neurite to branch. The direction of neurite outgrowth is also determined by extracellular signals to the growth cone (Tessier-Lavigne and Goodman, 1996).

Microtubule cytoskeleton

Tubulin is a molecule that when polymerized forms rigid microtubules which bundle together to give the internal skeleton of a neurite. Tubulin is produced in the soma and transported to the tip of the neurite (growth cone) by diffusion and active transport. At the growth cone the tubulin molecules are added to the end of the rod-like microtubules, extending their length (Kobayashi and Mundel, 1997). This assembly of tubulin into microtubules elongates the neurite. The individual microtubules are bundled together to form a rigid cytoskeleton. Branching within the terminal area can be facilitated by the destabilization of the microtubule bundles, when the bonds that tightly bind the microtubules together are relaxed, allowing the microtubules to separate and move in different directions (Maccioni and Cambiazo, 1995; Kobayashi and Mundel, 1997).

Microtubule assembly and bundling are regulated by microtubule-associated proteins (MAPs). MAP-2, for example, is a specific protein in this family found in dendrites. A major function of MAP-2 in the growing dendrite is to bind to the microtubules and stabilize them, thus promoting microtubule assembly and linking them together into bundles (Maccioni and Cambiazo, 1995; Kobayashi and Mundel, 1997). This stabilizing ability depends on the phosphorylation state of the MAP-2 molecules. Dephosphorylated MAP-2 favors growth as it promotes the assembly and bundling of microtubules. Phosphorylated MAP-2 is more likely to create branching conditions as the microtubule binding is relaxed and they become spaced further apart and are therefore easier to be forced apart by factors such as stress on the growth cone (Friedrich and Aszódi, 1991; Audesirk et al., 1997).

Calcium levels indirectly affect the rate of elongation and branching in a growing neurite. The rate at which MAP-2 is phosphorylated is regulated by calcium via a number of biochemical pathways (Hely et al., 2001). Factors that change the calcium level, such as electrical activity as the result of synaptic input, thus can also influence neurite outgrowth (Lohmann et al., 2002).

Growth cone

The growth cone is a structure at the tip of a neurite that plays an active role in the elongation and branching of a developing neurite. It can process external cues from the environment and turn this into useful action in terms of guiding the direction of neurite outgrowth. The growth cone can pull the tip of the neurite along or in separate directions, promoting either elongation or branching (van Veen and van Pelt, 1992; Li et al., 1994; Aeschlimann, 2000).

The growth cone contains an actin cytoskeleton, which adds mechanical strength to the cone, keeping its shape, and also helps drive and guide the cone's movement. Filopodia are small actin filament bundles extruding from the tip of the growth cone (see Fig. 1). These filopodia grow and retract at a high rate, probing the environment continuously, picking up guidance cues. Filopodia can adhere to the substrate, producing tension within the growth cone. Polymerization of actin filaments at the periphery of the growth cone and depolymerization centrally

effectively results in actin bundles moving backward through the growth cone, giving the growth cone a caterpillar track style movement (Li et al., 1994). The space that is created behind the growth cone by this pulling action is filled by microtubules and elongation occurs.

It has been hypothesized that when the filopodia are attached to the substrate they can produce enough tension to pull the actin cytoskeleton apart (Wessells and Nuttall, 1978; van Veen and van Pelt, 1992; Li et al., 1995). This will occur if the filopodia have found more than one guidance cue so that tension is applied to the growth cone in different directions. If this tension is great enough to overcome the structural strength of the cytoskeleton, the growth cone may split into two separate cones, with each following their own guidance cues.

Modeling neurite outgrowth

In the following sections we will review mathematical models of neurite outgrowth that attempt to capture biophysical aspects of neurite initiation, elongation, and branching. Typically such models concentrate on a particular aspect of neurite outgrowth, with an emphasis either on the intracellular or extracellular biophysics. Such a classification of the models is given in Table 1.

Intracellular models typically only seek to reproduce realistic neurite topologies, in terms of the number of terminals and the lengths of terminal and intermediate segments. The actual shape of the neurite in two- or three-dimensional space is not considered. An exception is the model of neurite initiation by Hentschel and Fine (1994, 1996) which generates neurite outgrowth in a two-dimensional plane due to intracellular instabilities. Extracellular models also produce neuronal shape. The models reviewed here only consider two-dimensional environments, which are equivalent to growing neurons in culture. Modeling growth in vivo would require a three-dimensional environment. This has been achieved in the nonbiophysical, stochastic L-system work of Ascoli and colleagues (Ascoli, 2002), but presents great computational demands for biophysically-based models.

In addition, models of neurite outgrowth can be classified according to the mathematical techniques they employ. Typically either ordinary differential equations (ODEs) or partial differential equations (PDEs) specify the growth model. A coupled set of ODEs specifies the dynamics of quantities at particular points within the growing neurite, typically the cell body, branch points, and terminals. PDEs specify values at all spatial locations. In either case, results are produced by numerical integration using finite difference schemes. The proper formulation of appropriate finite difference schemes is complicated by the changing morphology of a growing neurite, leading to free and moving boundary problems. This led Hentschel and Fine (1994, 1996) to use a cellular automata approach to designate regions as being inside, outside, or forming the membrane of a neuron. Consideration of numerical techniques is given below. Certain models are also amenable to

Table 1. Model classification by type

	Intracellular	Extracellular
Initiation	Hentschel and Fine (1994, 1996) Samuels et al. (1996)	
Elongation	Li et al. (1994) Miller and Samuels (1997) McLean et al. (2004) van Ooyen et al. (2001) van Veen and van Pelt (1994)	van Veen and van Pelt (1992) Li et al. (1992) Li et al. (1995)
Branching	Hely et al. (2001) Van Pelt et al. (2003)	van Veen and van Pelt (1992) Li et al. (1992) Li et al. (1995)

Table 2. Model classification by mathematical techniques

ODE	Samuels et al. (1996)
	Li et al. (1992)
	Li et al. (1994)
	Li et al. (1995)
	Miller and Samuels (1997)
	van Ooyen et al. (2001)
	van Pelt et al. (2003)
	van Veen and van Pelt (1992)
	van Veen and van Pelt (1994)
PDE	Hely et al. (2001)
	Hentschel and Fine (1994, 1996)
	McLean et al. (2004)
	Kiddie et al. (2004)
Cellular automata	Hentschel and Fine (1994, 1996)

analysis (Hentschel and Fine, 1994; van Veen and van Pelt, 1994; McLean et al., 2004). Classification of models according to their mathematical formulation is shown in Table 2.

Compartmental modeling

Mathematical modeling of neuronal properties often involves calculating quantities that vary over the spatial extent of the neuron. This is usually achieved by a one-dimensional spatial discretization of the tree structure formed by dendrites and the axon. When the quantity of interest is membrane voltage, this method has become known as compartmental modeling (see e.g., Koch and Segev, 1998). Techniques for specifying an appropriate compartmentalization (or discretization) for accurate calculation of voltage are well established.

Models that deal with the biophysics of neurite outgrowth typically are concerned with the concentration of chemicals, both intra- and extracellularly, that determine growth. Intracellular PDE models use a similar one-dimensional discretization to compartmental modeling of voltage. A difficulty arises, however, in that the cell morphology changes over time, necessitating continual respecification of the discretization.

Fixed compartment number

Numerical solution of a PDE model of neurite elongation by means of finite differences (McLean et al., 2004) yields a compartment model which contains a fixed number of compartments, regardless of the neurite's length. This is achieved via a spatial transformation of the model so that spatial values are always solved over a [0,1] length domain. Values are calculated at N different points within this domain, where N is the number of compartments. As the actual neurite length changes over time, so the real spatial locations (or, equivalently, the size of the compartments) of the N values changes, as illustrated in Fig. 2.

For numerical stability it is important that the number of compartments, N, is sufficient for the discretization of the maximum expected length. This may be an unnecessarily large number for the early stages of growth when the length is short.

The fact that the compartments are not positionally static may also be problematic for modeling particular situations. For example, modeling synapse formation during neurite outgrowth and the subsequent response of the neuron to synaptic input requires that the exact spatial location of the synapse be stationary.

Fixed compartment size

An alternative discretization scheme keeps the size of most compartments fixed and allows the addition of new compartments. A number of variations on how neurite elongation and branching are handled with such a scheme are possible (Graham and van Ooyen, 2001). The most numerically satisfactory approach is illustrated in Fig. 3. Here, all but the single compartments immediately preceding branch terminals (growth cones) remain of fixed size, dx. Growth is handled by elongating these preceding compartments. When their length exceeds $2 \times dx$ they are divided into two compartments, the most proximal of which is given the fixed length dx, with the distal compartment retaining the remaining length. It is also the one that continues elongating.

In this scheme, most discrete points at which chemical concentrations are calculated are positionally static. This may be advantageous for modeling neurite interaction with the external environment, including contact and synapse formation with other neurites. However, specifying a single compartment

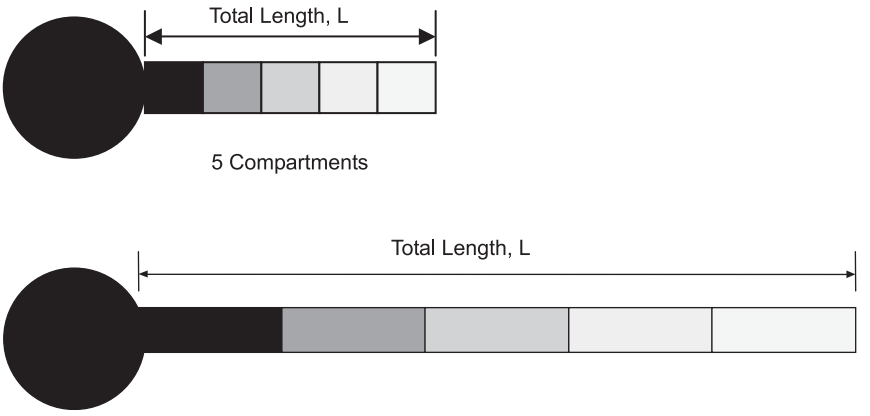

Fig. 2. Discretization of elongation model. Top: early time. Bottom: later time.

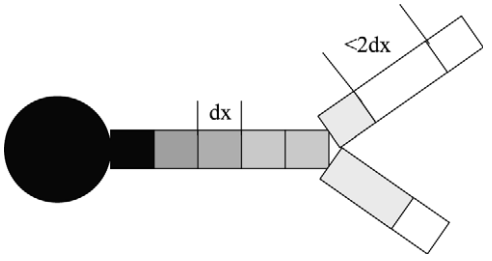

Fig. 3. Fixed size compartment model.

size, dx, is inefficient. A size that is small enough for accurate calculation in short neurite branches may lead to older, longer branches being described by an unnecessarily large number of compartments with a resultant high computational load for numerical simulation. Both this *fixed compartment size* and the *fixed compartment number* approaches to spatial discretization thus are not optimal in particular situations, but both provide practical solutions. The fixed size scheme has been used to implement detailed elongation and branching models that rely on accurate calculation of chemical concentrations in terminal compartments (Hely et al., 2001; Kiddie et al., 2004).

Other solution methods

Methods other than those of finite differences exist for the solution of PDEs, most notably the finite element methods or the spectral methods. Ostensibly, the finite element method can be thought of as a natural generalisation of finite differences (see, e.g., Burnett, 1987). A spectral method, on the other hand, approximates the solution $u(x,t)$ to a PDE by a truncated series

$$u^N(x,\,t) = \sum_{j=1}^{N} \hat{u}_j \varphi_j(x) \quad \text{on } x \in [a,b],\ a < b.$$

Here, N is the truncation size, $\varphi_j(x)$ is the trial function ($j = 1, 2, \ldots$) orthogonal over $[a,b]$ and $\hat{u}_j(t)$ are the time-varying coefficients. The trial functions could be the trigonometric polynomials if a periodic solution is sought, but in the case of neurite growth, a more appropriate set of orthogonal polynomials would be the Chebyshev polynomials

$$\varphi_j(x) \equiv T_j(x) = \cos(\, j \cos^{-1} x)$$

which are defined on $[-1, 1]$ (a simple transformation would render them useful on the unit interval $[0, 1]$). In a numerical solution by means of expansion in Chebyshev polynomials, the problem becomes one of solving for the coefficients $\hat{u}_j(t)$ rather than function values at a discrete set of points. The spectral method has been used extensively in solving the equations of fluid dynamics and elegant treatments are given in the books by Canuto et al. (1988) and Boyd (1989).

In employing a spectral method, we do away with the idea of compartments, focussing in on solving for the coefficients in a truncated series expansion. In this

way, the problem of locating the correct compartment during simulated synapse formation or neurite–neurite contact can be circumvented. The inclusion of a Dirac-delta function in the source/degradation term at the site of synapse formation could then be included in the equations governing the concentration evolution of intracellular proteins without recourse to identifying any non-physical ''compartment.''

Two-dimensional internal and external environments

Hentschel and Fine (1994, 1996) employ an explicit two-dimensional discretization of the intracellular space, which is divided into 1 μm^2 pixels. Individual pixels either belong to the cytoplasm or to the membrane of the neuron. The membrane is treated as being one pixel thick. Extracellular space is simply regarded as well-mixed, so explicit extracellular pixels are not required. Diffusion of chemicals in the cytoplasm and across the membrane is modelled. Growth of the neuron requires addition and deletion of membrane. In a cellular automata approach, a stochastic growth rule is applied at each time step to membrane pixels to decide whether they should be deleted (retraction) or whether new membrane pixels should be added in the neighbourhood (growth).

Models that consider the external environment in which the neurite is growing typically represent this as a two-dimensional space. The space can contain morphogen gradients that influence the direction and extent of neurite outgrowth (Li et al., 1992, 1994, 1995; van Veen and van Pelt, 1992; Hentschel and van Ooyen, 1999). Morphogen gradients can be specified functionally, so that a fine discretization of the environment is not necessary. For example, concentration of a morphogen may decrease linearly in one spatial dimension, or be restricted to particular geometric areas, such as rectangular bands (Li et al., 1992, 1994, 1995). The quasi-steady-state diffusion gradient of a morphogen released from a point source can be calculated (Hentschel and van Ooyen, 1999). van Veen and van Pelt (1992) randomly distribute discrete adhesion sites and consider the density of such sites in a detection area preceding a growth cone. The spatial location of individual neurites can also be tracked, so that the effect of neurite-to-neurite contact can be modelled (Li et al., 1992, 1995).

Neurite initiation and differentiation

Intracellular calcium affects neurite outgrowth (Kater et al., 1988; Goldberg and Grabham, 1999). Deviations in either direction from an optimal calcium concentration slow down neurite elongation and can even cause retraction. Hentschel and Fine 1994, 1996; (for a review, see Hentschel and Fine (2003)) have shown that this dependence of growth on calcium can lead to the emergence of dendritic forms from initially spherical cells. In their model, local outgrowth of the cell membrane is taken to depend on the local concentration of calcium close to the internal surface of the membrane. Local calcium concentration results from influx, extrusion, and diffusion. Because of the larger surface to volume ratio, the local calcium concentration at spontaneously occurring small protrusions of the cell membrane will become higher that at other points of the membrane. These protrusions of the membrane will not decay because of the existence of a positive feedback loop. As a consequence of the presence of voltage sensitive calcium channels and the influence of calcium on the membrane potential, calcium influx increases with increased local calcium concentration. Provided that the calcium concentration does not become too high, this will lead to continued outgrowth of the protrusions. The growth of cells in their model resembles the dynamic behaviour of growing neurons. In both model neurons and natural neurons, initial outgrowth consists of broad, irregular extensions and short, very fine extensions of the cell membrane. Distinct processes (neurites) emerge only subsequently. These processes spontaneously form enlargements at their actively growing tips, which in turn give rise to branches. In both model and natural neurons, small processes often retract, and the extension of large processes may be punctuated by episodes of stasis or retraction.

The differentiation of neurites into axon and dendrites may also involve some positive feedback loop. During neuronal outgrowth, one of the neurites rapidly increases its growth rate, becoming differentiated as the axon, while the growth rates of the

other neurites are reduced. Axotomy experiments have shown that all neurites have the potential to develop into axons (Dotti and Banker, 1987; Goslin and Banker, 1989). When the axon is cut during development, the longest remaining neurite differentiates into the new axon. If the two longest neurites are roughly of equal length, then it takes longer to decide which neurite becomes the new axon. Samuels et al. (1996) have shown that a winner-take-all dynamic instability can explain a great deal of the experimental data about axonal differentiation. In their model, there is a single chemical that determines the rate of growth of the neurites. This determinant chemical is produced in the soma and is transported, by diffusion and active transport, to the tips of the growing neurites, where it is consumed by the growth process. For a unique axon to develop, they found that it was necessary to assume that the active (anterograde) transport should increase with the growth rate of the neurite. They propose that a possible biological mechanism for this positive feedback loop is that an increased growth rate would pull more cytosol into the neurite's proximal end, where there is access to the transport mechanism. The numerical simulation of their model shows an instability leading to the formation of a single fast growing neurite, identified as the axon, with the rest of the neurites growing very slowly. The model also explains, at least qualitatively, the various axotomy experiments.

Elongation

A family of models has considered neurite elongation as determined by the production and transport of tubulin along the neurite and subsequent microtubule assembly at the neurite tip (van Veen and van Pelt, 1994; Miller and Samuels, 1997; van Ooyen et al., 2001; McLean et al., 2004).

The work of Miller and Samuels (1997) attempted to explain the steady state or maximal lengths in axonal growth under the so-called slow transport mechanism. The hypothesis was that axonal length is limited by the distance degrading cytoskeletal proteins can be transported. In a simple model of protein transport, Miller and Samuels (1997) described the mechanisms of protein flux and protein degradation with a single ODE which was subsequently considered only in the steady state. They used a specifically simple form for the flux being the product of the average, or apparent, transport velocity and the protein concentration. Arguing that the protein concentration was constant along the length of a mature axon, they were able to find maximal lengths in the steady state. Their model was verified against a number of data for slow transport in various animal axons. The simplicity of their model even allowed them to track, with some success, the peak of a labelled protein distribution taken from the work of Hoffman and Lasek (1975).

The limiting effects of tubulin transport on the dynamics of neurite elongation have also been investigated in simple ODE models (van Veen and van Pelt, 1994; van Ooyen et al., 2001). A constant elongation rate results if tubulin transport is by diffusion only and tubulin degradation is sufficiently slow that it can be neglected (van Veen and van Pelt, 1994). Variation in transport and particularly in microtubule (dis)assembly rates between neurite branches leads to competitive growth in which particular neurites may obtain more of the finite tubulin resource. A dominant branch can restrict outgrowth of other branches. If a dominant branch stops growing, for example due to forming a synaptic connection, the tubulin concentration in the other growth cones increases, thus facilitating the outgrowth of previously dormant branches (van Ooyen et al., 2001).

In a generalisation of the above models, McLean et al. (2004) took a conservation law approach for the concentration of tubulin. Mechanisms of active molecular transport, diffusion, and degradation led to a spatio-temporal continuum PDE model for the bulk or average tubulin concentration and neurite length. Under this model, the growth of a neurite begins with the production of tubulin at the cell body, its displacement to the growth tip followed by its polymerization onto the microtubules at the growth tip. The model is mathematically challenging since it is of the moving boundary type. A spatial transformation that introduced nonlinearities to the tubulin governing equation rendered the growth domain fixed. McLean et al. (2004) then sought steady state solutions which lead to the derivation of

a transcendental equation for the steady state length. Having identified a key parameter grouping, they found three different regimes for small, intermediate, and large steady state neurite lengths. In fact, it was established that a neuron could easily regulate the extent of its neurites by simply modulating the tubulin production at the soma relative to the active transport/degradation fraction. An eigenvalue analysis and stability analysis of the unsteady problem is currently underway to ascertain the stability of these steady state solutions. Numerical solutions of the model (McLean et al., 2004) reveal that oscillations in neurite length may appear in the transition from small to large growth.

In the models described above, neurite elongation due to external effects, such as tension on the growth cone, are not considered. Models of branching due to tension on filopodia also determine elongation rates on the basis of this tension (Li et al., 1992, 1995; van Veen and van Pelt, 1992). Li et al. (1994) examined a system of growth cone locomotion based upon actin polymerization and growth cone adhesion. This is similar to microtubule assembly in the trailing neurite, but concentrated upon the construction of the actin cytoskeleton in the growth cone. Filopodia are not explicitly modelled. The leading edge of the growth cone is assumed to adhere to the substrate. Assembly of actin filaments at the leading edge and disassembly at the transition from the growth cone to the neurite results in caterpillar-style forward movement of the growth cone due to traction forces.

Related models are more concerned with the direction of neurite outgrowth, rather than the mechanisms generating elongation. Of particular importance here is understanding how cues in the environment can guide axons over long distances to their appropriate targets (Hentschel and van Ooyen, 1999; Aeschlimann, 2000; Goodhill, 2003).

Mathematical models can also be used to examine the microscopic phenomena underlying these growth models. Smith and Simmons (2001) consider scenarios for motor-assisted (active) transport of organelles. The microscopic dynamics of microtubule assembly have been modelled (Odde, 1997; Pedigo and Williams, 2002). Janulevicius et al. (2003) determine how the volume of a growth cone influences microtubule assembly within the cone.

Branching

Several papers consider neurite branching as a result of external tension applied to the growth cone (Li et al., 1992, 1995; van Veen and van Pelt, 1992). In these models, filopodia extending from the leading edge of the growth cone adhere to the substrate in directions determined by attractive or repulsive cues in the environment. If all the filopodia pull in the same direction, the neurite elongates. However, filopodia on opposite sides of the growth cone may find attractive cues in different directions, resulting in tension on the growth cone. If this tension overcomes a preset threshold then branching occurs by splitting of the growth cone. The tension threshold is implicitly determined by the state of the actin cytoskeleton within the growth cone. These models differ in detail concerning the specification of filopodia and cues in the external environment. Li et al. (1992, 1995) also introduce an implicit intracellular mechanism by which the outgrowth of a neurite inhibits the growth of other neurites from the same cell. This could be due to competition for available tubulin, as explicitly investigated in the elongation models described above (van Veen and van Pelt, 1994; van Ooyen et al., 2001).

Branching is also in part determined by the construction and stability of the microtubule cytoskeleton in the trailing neurite. Several models have investigated the neurite morphologies that result if branching is rate-limited by the availability of a resource, such as free tubulin, at neurite terminals (Graham et al., 1998; van Pelt et al., 2003) If this resource is produced in the cell body and is transported by diffusion and active transport to the terminals, the branching rate is modulated both with the number of terminals in the growing tree and their centrifugal order (number of branch points between a terminal and the cell body). This is similar to the branching dependencies of real neurites, revealed by statistical models of neurite outgrowth (van Pelt et al., 1997; van Pelt and Uylings, 1999).

A model of elongation and branching as modulated by the effects of MAP-2 on the construction of the microtubule cytoskeleton has been proposed in Hely et al. (2001). In this model, the rates of elongation and branching were in part determined by the rate of binding, unbinding, and

phosphorylation of MAP-2. Binding of unphosphorylated MAP-2 to microtubules at a neurite tip increased the rate of microtubule assembly and stabilized the microtubule bundles, leading to faster elongation and a lower rate of branching. Phosphorylation of the MAP-2 disrupted its stabilizing function and promoted branching. The rate of phosphorylation was controlled by the local calcium concentration. Changes in calcium concentration during outgrowth, and the precise relationship between calcium and MAP-2 phosphorylation, determined the resultant branched tree morphology.

New model of elongation and branching

Here we describe a new model that incorporates the effects of MAP-2 on the construction of the microtubule cytoskeleton (Kiddie et al., 2004). This effectively combines the microtubule-based elongation models with the MAP-2 model of Hely et al., (2001). Tubulin and MAP-2 are produced in the cell body and transported by active transport and diffusion to the neurite tips. Calcium influx occurs along the length of the neurite and calcium can diffuse internally. Neurite elongation is a function of the microtubule assembly rate, which depends on the available tubulin and is modulated by bound (unphosphorylated) MAP-2. The terminal branching probability is a function of the relative amount of phosphorylated MAP-2.

The equations for each of the three chemicals, tubulin, MAP-2 and calcium, are given below. They are presented in the form of a first-order discretization of the underlying PDE model that is equivalent to the compartment structure illustrated in Fig. 3. The model neurite is separated into the soma, the intermediate compartments, and the terminal compartments. The soma has a simple *production/influx–transport–decay* structure for each chemical. The intermediate compartments have a *transport in–transport out–decay* structure. Terminal compartments are more complicated. The calcium retains its influx–diffusion–decay structure. Tubulin is still transported and may decay, but is now also affected by assembly and disassembly to and from microtubules. The unbound MAP-2 still diffuses and decays, but may now bind to microtubules. The bound MAP-2 is affected by decay and its phosphorylation rate, which is a function of calcium.

Soma

Tubulin

$$\begin{aligned}\frac{dT_0}{dt} &= P + \frac{\hat{D}(T_1 - T_0)}{dx} - \eta T_0 - \delta_t T_0 \\ &= \text{Production} + \text{Diffusion} - \text{Active transport} \\ &\quad - \text{Decay}\end{aligned}$$

Unbound MAP-2

$$\begin{aligned}\frac{dU_0}{dt} &= S + \frac{\hat{D}(U_1 - U_0)}{dx} - \delta_u U_0 \\ &= \text{Production} + \text{Diffusion} - \text{Decay}\end{aligned}$$

Calcium

$$\begin{aligned}\frac{dC_0}{dt} &= I + \frac{\hat{D}(C_1 - C_0)}{dx} - \delta_c C_0 \\ &= \text{Influx} + \text{Diffusion} - \text{Decay}\end{aligned}$$

Intermediate

Tubulin

$$\begin{aligned}\frac{dT_i}{dt} &= \frac{\hat{D}(T_{i+1} - T_i)}{dx} + \frac{\hat{D}(T_{i-1} - T_i)}{dx} \\ &\quad + \eta T_{i-1} - \eta T_i - \delta_t T_i \\ &= \text{Diffusion} + \text{Active transport in} \\ &\quad - \text{Active transport out} - \text{Decay}\end{aligned}$$

Unbound MAP-2

$$\begin{aligned}\frac{dU_i}{dt} &= \frac{\hat{D}(U_{i+1} - U_i)}{dx} + \frac{\hat{D}(U_{i-1} - U_i)}{dx} - \delta_u U_i \\ &= \text{Diffusion} - \text{Decay}\end{aligned}$$

Calcium

$$\frac{dC_i}{dt} = I + \frac{\hat{D}(C_{i-1} - C_i)}{dx} + \frac{\hat{D}(C_{i+1} - C_i)}{dx} - \delta_c C_i$$
$$= \text{Influx} + \text{Diffusion} - \text{Decay}$$

Terminal

Tubulin

$$\frac{dT_t}{dt} = \frac{\hat{D}(T_{t-1} - T_t)}{dx} + \eta T_{i-1} - \delta_t T_t - \varepsilon_t T_t B_t + \psi_t$$
$$= \text{Diffusion} + \text{Active transport in} - \text{Decay} - \text{Assembly} + \text{Disassembly}$$

Calcium

$$\frac{dC_t}{dt} = I + \frac{\hat{D}(C_{t-1} - C_t)}{dx} - \delta_c C_t$$
$$= \text{Influx} + \text{Diffusion} - \text{Decay}$$

Unbound MAP-2

$$\frac{dU_t}{dt} = \frac{\hat{D}(U_{t-1} - U_t)}{dx} - \delta_u U_t - c_1 U_t + c_2 B_t$$
$$= \text{Diffusion} - \text{Decay} - \text{Binding} + \text{Unbinding}$$

Bound (unphosphorylated) MAP-2

$$\frac{dB_t}{dt} = c_1 U_t - c_2 B_t - c_3 F B_t + c_4 G P_t - \delta_b B_t$$
$$= \text{Binding} - \text{Unbinding} - \text{Phosphorylation} + \text{Dephosphorylation} - \text{Decay}$$

Phosphorylated MAP-2

$$\frac{dP_t}{dt} = c_3 F B_t - c_4 G P_t - \delta_p P_t$$
$$= \text{Phosphorylation} - \text{Dephosphorylation} - \text{Decay}$$

Elongation

$$\frac{dL}{dt} = \varepsilon_t T_t B_t - \psi_t$$
$$= \text{Microtubule assembly} - \text{Disassembly}$$

Branching probability

$$B_{\text{PR}} = k_B \frac{P_t}{P_t + B_t} = \text{Probability of branching}$$

Calcium Rate Converters

$$F = \frac{C_t^2}{k_F + C_t^2} = \text{Phosphorylation rate limit}$$

$$G = \frac{C_t^2}{k_G + C_t^2} = \text{Dephosphorylation rate limit}$$

Parameters

Initial results with this model illustrate that it can produce a variety of different types of neuritic tree morphology with small changes in parameter values. There are three sets of parameters used during the simulations: an initial set and two modified sets that generate alternative tree topologies (Table 3).

The model is simulated by calculating the concentration of each chemical in all compartments at each time step, and performing compartment elongation and branching as necessary, using the *fixed compartment size* approach (see Compartmental modeling section). All chemical concentrations start at zero. Simple first-order Euler approximations over time and space are used to discretize the equations, as shown above. The model is implemented in MATLAB.

Results

The results in Fig. 4 show that the model can produce several different tree topologies with minimal changes to the parameters. The initial tree type displays a relatively uniform segment length throughout the tree (Fig. 4a). The other tree types have long intermediate segments with short terminal segments (Fig. 4b) or relatively long terminal segments (Fig. 4c). These tree types are consistent with similar topologies produced by Hely's MAP-2 model (Hely et al., 2001) and statistical information from real neuronal trees (van Pelt and Uylings, 1999).

Figure 5 shows the differences in terminal segment and intermediate segment lengths, with the changes in

Table 3. (a) Parameter values for normal tree (b) Changes that give short terminals (c) Changes that give long terminals

Parameters	Normal tree	Short terminals	Long terminals
Calcium influx (I)	0.3		
Decay of calcium (δ_c)	0.01		
Tubulin production (P)	0.7		
Decay of tubulin (δ_t)	0.01		
Unbound MAP-2 production (S)	0.5		
Decay of unbound MAP-2 (δ_u)	0.3		
Active transport rate (η)	0.3		
Tubulin assembly rate (ε_t)	0.1		
Tubulin disassembly rate (ψ_t)	0.0005		
Decay phosphorylated MAP-2 (δ_p)	0.5		
Decay of bound MAP-2 (δ_b)	0.3		
Conversion constant 1 (c_1)	0.4	0.2	0.5
Conversion constant 2 (c_2)	0.3	0.5	0.2
Conversion constant 3 (c_3)	0.4	0.5	0.2
Conversion constant 4 (c_4)	0.3	0.2	0.5
Calcium rate constant (k_F)	0.5		
Calcium rate constant (k_G)	0.5		
Branching constant (k_B)	0.01		
Diffusion constant (D)	0.3		

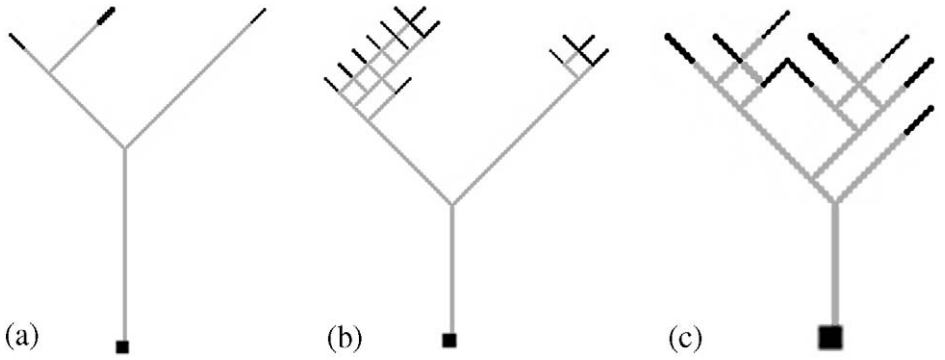

Fig. 4. Examples of tree topology for trees with (a) Similar intermediate and terminal lengths (Normal model), (b) Long intermediate and short terminals, (c) Short intermediate and long terminals.

parameter values. The histograms display data from 100 simulated trees for each of the topologies shown in Fig. 4.

The differences between the three topologies have been generated by changing the rate constants that dictate how much MAP-2 converts to and from its unbound, bound, and phosphorylated states. By increasing the rate at which bound MAP-2 is converted into phosphorylated MAP-2 (Constant 3) and reducing the rate at which phosphorylated MAP-2 is turned back into bound MAP-2 (Constant 4), the average amount of phosphorylated MAP-2 increases. This is accentuated by limiting the amount of MAP-2 that becomes bound to microtubules (Constants 1 and 2). This raises the probability of branching and results in longer intermediate segments and shorter terminal segments, as can be seen in Figs. 4b and 5b. Decreasing the rate at which bound MAP-2 is converted into phosphorylated MAP-2 (Constant 3) and increasing the rate at which phosphorylated MAP-2 is turned back into bound MAP-2 (Constant 4), reduces the amount of phosphorylated MAP-2 and branching decreases. The amount of bound MAP-2 is also raised by an increase in the binding rate from unbound MAP-2 (Constants 1 and 2). This promotes elongation and results in shorter

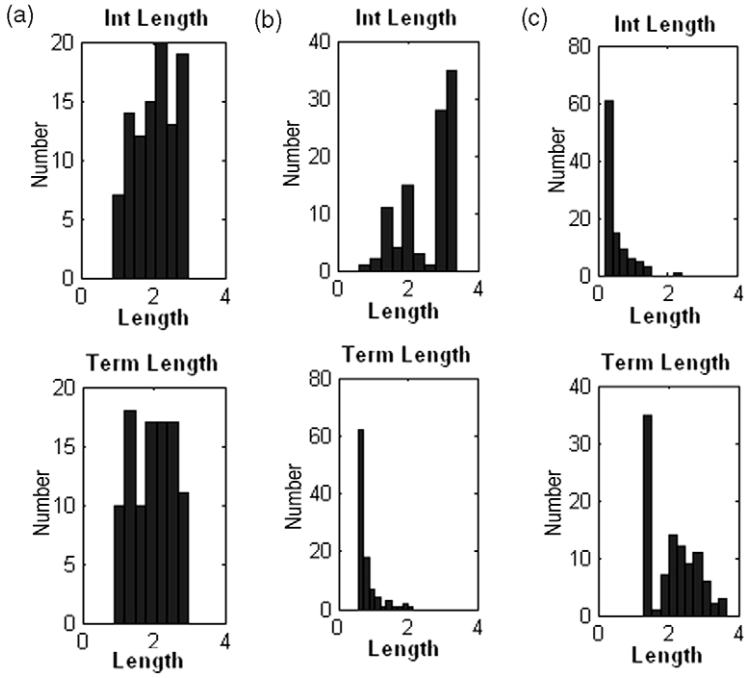

Fig. 5. Histograms of segment lengths from 100 simulated trees for with (a) Similar intermediate and terminal lengths (Normal model), (b) Long intermediate and short terminals, (c) Short intermediate and long terminals.

intermediate segments and longer terminal segments, as can be seen in Figs. 4c and 5c.

Further work with this model will investigate the influence of the production and transport of tubulin and MAP-2 on tree morphology. Calcium concentration plays a key role in setting MAP-2 (de)phosphorylation rates, and changes in calcium concentration in terminals during outgrowth will affect elongation and branching rates (Hely et al., 2001). Consequently, the effects of calcium influx and diffusion need to be studied. Calcium-induced calcium release may need to be modeled as this has been shown to play a role in stabilizing neurite branches during development (Lohmann et al., 2002). Parameter values will be derived from experimental data, where possible.

Conclusions

Mathematical modeling and computer simulation have a valuable role to play in understanding the processes driving morphological development in neurons. To date a variety of models based on particular biophysical aspects of neuronal development have shed light on neurite initiation, differentiation, elongation, and branching. These models provide an excellent platform on which to build new, more complex models that combine aspects of the biophysics and attempt to include the latest experimental data. We have described the initial formulation and results from one such model that examines neurite development as driven by the construction of the microtubule cytoskeleton. This model will eventually be extended to include a realistic growth cone, with an actin cytoskeleton and physical interaction with an explicit external environment.

Acknowledgments

This work has been funded by EPSRC grant GR/R89769/01 to BPG.

References

Acebes, A. and Ferrus, A. (2000) Cellular and molecular features of axon collaterals and dendrites. TINS, 23: 557–565.

Aeschlimann, M. (2000) Biophysical Models of Axonal Pathfinding. Ph.D. Thesis, University of Lausanne, Faculty of Science, Switzerland.

Ascoli, G. (2002) Neuroanatomical algorithms for dendritic modeling. Network: Comput. Neural Syst., 13: 247–260.

Audesirk, G., Cabell, L. and Kern, M. (1997) Modulation of neurite branching by protein phosphorylation in cultured rat hippocampal neurons. Developmental Brain Research, 102: 247–260.

Boyd, J.P. (1989) Chebyshev and Fourier Spectral Methods. Springer-Verlag, New York.

Burnett, D.S. (1987) Finite Element Analysis: From Concepts to Applications. Addison-Wesley, Reading, MA.

Canuto, C., Hussaini, M.Y., Quarteroni, A. and Zhang, T.A. (1988) Spectral Methods in Fluid Dynamics. Springer Verlag, New York.

Cline, H. (2001) Dendritic arbor development and synaptogenesis. Current Opinion in Neurobiology, 11: 118–126.

Dehmelt, L. and Halpain, S. (2004) Actin and microtubules in neurite initiation: are MAPs the missing link? J. Neurobiol., 58: 18–33.

Dotti, C.G. and Banker, G.A. (1987) Experimentally induced alterations in the polarity of developing neurons. Nature, 330: 254–256.

Dotti, C.G., Sullivan, C.A. and Banker, G.A. (1988) The establishment of polarity by hippocampal neurons in culture. J. Neurosci., 8: 1454–1468.

Friedrich, P. and Aszódi, A. (1991) MAP2: a sensitive cross-linker and adjustable spacer in dendritic architecture. FEBS, 295: 5–9.

Goldberg, D.J. and Grabham, P.W. (1999) Braking news: calcium in the growth cone. Neuron, 22: 423–425.

Goodhill, G.J. (2003) A theoretical model of axon guidance by the robo code. Neur. Comput., 15: 549–564.

Goslin, K. and Banker, G. (1989) Experimental observations on the development of polarity by hippocampal neurons in culture. J. Cell Biol., 108: 1507–1516.

Graham, B., Hely, T. and van Ooyen, A. (1998) An internal signalling model of the dendritic branching process. Euro. J. Neurosci, 10(Supplement 10): 274.

Graham, B. and van Ooyen, A. (2001) Compartmental models of growing neurites. Neurocomputing, 38–40: 31–36.

Hely, T., Graham, B. and van Ooyen, A. (2001) A computational model of dendritic elongation and branching based on MAP-2 phosphorylation. J. Theor. Biol, 210: 375–384.

Hentschel, H.G.E. and Fine, A. (1994) Instabilities in cellular dendritic morphogenesis. Phys. Rev. Lett., 73: 3592–3595.

Hentschel, H.G.E. and Fine, A. (1996) Diffusion-regulated control of cellular dendritic morphogenesis. Proc. R. Soc. B, 263: 1–8.

Hentschel, H.G.E. and van Ooyen, A. (1999) Models of axon guidance and bundling during development. Proc. R. Soc. B, 266: 2231–2238.

Hentschel, H.G.E. and Fine, A. (2003) Early dendritic and axonal morphogenesis. In: van Ooyen A. (Ed.), Modeling Neural Development. MIT Press, Cambridge, MA, pp. 49–74.

Hoffman, P.N. and Lasek, R.J. (1975) The slow component of axonal transport, identification of major structural polypeptides of the axon and their generality among mammalian neurons. J. Cell Biol., 66: 351–366.

Janulevicius, A., van Pelt, J. and van Ooyen, A. (2003) The effect of dynamic instability of microtubules on growth cone dynamics. Computational Neuroscience Meeting. Alicante, Spain.

Kater, S.B., Mattson, M.P., Cohan, C. and Connor, J. (1988) Calcium regulation of the neuronal growth cone. Trends in Neurosci., 11: 315–321.

Kiddie, G.A., Graham, B.P. and van Ooyen, A. (2004) Biologically plausible model of growing neurites. Brain-Inspired Cognitive Systems. Stirling, U.K., in press.

Kobayashi, N. and Mundel, P. (1997) A role of microtubules during the formation of cell processes in neuronal and non-neuronal cells. Cell tissue Res., 291: 163–174.

Koch, C. and Segev, I. (1998) Methods of Neuronal Modeling: From Ions to Networks. MIT Press, Cambridge, MA.

Li, G., Qin, C. and Wang, Z. (1992) Neurite branching pattern formation: modeling and computer simulation. J. Theor. Biol., 157: 463–486.

Li, G., Qin, C. and Wang, Z. (1994) On the mechanisms of growth cone locomotion: modeling and computer simulation. J. Theor. Biol., 169: 255–362.

Li, G., Qin, C. and Wang, Z. (1995) Computer model of growth cone behavior and neuronal morphogenesis. J. Theor. Biol., 174: 381–389.

Lohmann, C., Myhr, K.L. and Wong, R.O.L. (2002) Transmitter-evoked local calcium release stabilizes developing dendrites. Nature, 418: 177–181. doi:10.1038/nature00850.

Maccioni, R.B. and Cambiazo, V. (1995) Role of microtubule-associated proteins in the control of microtubule assembly. Physiological Reviews, 75: 835–857.

McLean, D., van Ooyen, A. and Graham, B. (2004) Continuum model for tubulin-driven neurite elongation. Neurocomputing, in press.

Miller, K. and Samuels, D. (1997) The axon as a metabolic compartment: protein degradation, transport and maximum length of an axon. J. Theor. Biol., 186: 373–379.

Odde, D.J. (1997) Estimation of the diffusion-limited rate of microtubule assembly. Biophysical Journal, 73: 88–96.

Pedigo, S. and Williams, R. (2002) Concentration dependence of variability in growth rates of microtubules. Biophys. J., 83(4): 1809–1819.

Redmond, L. and Ghosh, A. (2001) The role of Notch and Rho GTPase signalling in the control of dendritic development. Curr. Opin. Neurobiol., 11: 111–117.

Samuels, D.C., Hentschel, H.G.E. and Fine, A. (1996) The origin of neuronal polarization: a model of axon formation. Phil. Trans. R. Soc. B., 351: 1147–1156.

Smith, D.A. and Simmons, R.M. (2001) Models of motor-assisted transport of intracellular particles. Biophys. J., 80(1): 45–68.

Tessier-Lavigne, M. and Goodman, C.S. (1996) The molecular biology of axon guidance. Science, 274: 1123–1133.

van Ooyen, A., Graham, B. and Ramakers, G. (2001) Competition for tubulin between growing neurites during development. Neurocomputing, 38–40: 73–78.

van Pelt, J., Dityatev, A. and Uylings, H. (1997) Natural variability in the number of dendritic segments: model-based inferences about branching during neurite outgrowth. J. Comp. Neurol., 387: 325–340.

van Pelt, J., Graham, B. and Uylings, H. (2003) Formation of dendritic branching patterns. In: van Ooyen A. (Ed.), Modeling Neuronal Development, chapter 4. MIT Press, Cambridge, MA, pp. 75–94.

van Pelt, J. and Uylings, H. (1999) Natural variability in the geometry of dendritic branching patterns. In: Poznanski R.R. (Ed.), Modeling in the Neurosciences: From Ionic Channels to Neural Networks. Harwood Academic, Amsterdam, pp. 79–108.

van Veen, M. and van Pelt, J. (1992) A model for outgrowth of branching neurites. J. Theor. Biol., 159: 1–23.

van Veen, M.P. and van Pelt, J. (1994) Neuritic growth rate described by modeling microtubule dynamics. Bull. math. Biol., 56: 249–273.

Wessells, N.K. and Nuttall, R.P. (1978) Normal branching, induced branching, and steering of cultured parasympathetic motor neurons. Exp. Cell. Res., 115: 111–122.

Whitford, K., Dijkhuizen, P., Polleux, F. and Ghosh, A. (2002) Molecular control of cortical dendrite development. Ann. Rev. Neurosci., 25: 127–149.

Wong, W.T. and Wong, R.O.L. (2000) Rapid dendritic movements during synapse formation and rearrangement. Current Opinion in Neurobiology, 10: 118–124.